UNIVERSITI SAINS MALAYSIA

Laporan Akhir Projek Penyelidikan Jangka Pendek

Investigation Charge Conduction Mechanism in Metal-Organic Decomposition Derived Lanthanum Cerium Oxide Film

by
Lim Way Fong

2013

II. CONTENTS OF REPORT

1. ABSTRACT/SUMMARY OF REPORT

In this project, lanthanum cerium oxide ($La_xCe_{1-x}O_z$) was studied for two properties, which serve as a metal reactive oxide with catalytic behaviour for metal-oxide-semiconductor (MOS) based field effect gas sensor and a passivation layer possessing insulating behaviour in MOS based devices. To address these two properties, investigation was carried out by depositing the oxide on Si and 4H-SiC substrates and varying the post-deposition annealing temperature (400–1000°C), post-deposition annealing time (15–120 min), post-deposition annealing ambient (Ar, O_2, N_2, 95%N_2-H_2), spin-coating rate (3000, 4000, 5000 rpm), and molar ratio of La:Ce (1:1, 1:0.75, 1:0.50, 1:0.25, 1:0) in $La_xCe_{1-x}O_z$. Catalytic behaviour was successfully revealed through the addressing of carbon removal from the $La_xCe_{1-x}O_z$/4H-SiC interface, uncontrolled growth of SiO_x interfacial layer thickness at $La_xCe_{1-x}O_z$/Si interface, and catalytic oxidation of the 4H-SiC substrate surface starting from temperature as low as 400°C. Related mechanism has been proposed, demonstrated, and discussed in this project. The presence of catalytic behaviour in $La_xCe_{1-x}O_z$ was due to the redox characteristics of cerium cation in the oxide, which involves frequent exchange between the lattice oxygen and gas phase oxygen. Redox in $La_xCe_{1-x}O_z$ eventually formed oxygen vacancies as active sites for detection of gas molecules from the ambient. Sensing performance of Al/$La_xCe_{1-x}O_z$/Si and Al/$La_xCe_{1-x}O_z$/4H-SiC was studied and demonstrated. Higher the presence of oxygen vacancies in the structure, greater sensitivity was gained. In addition, to address $La_xCe_{1-x}O_z$ as a passivation layer in MOS based devices, electrical studies in terms of leakage current density-gate voltage and capacitance-gate voltage characteristics was carried out. $La_xCe_{1-x}O_z$ was a potential high dielectric constant (k) oxide due to the yield of high value of dielectric

constant as well as low leakage current density and high breakdown voltage comparable with other reported high *k* oxides deposited on either Si or 4H-SiC substrates.

2. Introduction

Recent development in gas sensors has gradually eliminated the tedious conventional analytical instruments, which include mass spectrometer, NMR and chromatography for the sake of the complexity, cost, and size. Sensing technology has then switched to using the solid-state field effect metal-oxide-semiconductor (MOS) gas sensors. Among the advantages include smaller size, high sensitivity, and low cost. Numerous researches have shown that a characteristic of solid-state field effect MOS gas sensors depend on the gate electrode and gate oxide. To-date, palladium, platinum, and nickel have been widely used as the gate electrode in field-effect MOS gas sensors due to the ability of these electrodes to absorb and dissolve the analyte gas. Silver gate has been also utilized as the potential gas electrode due to the high affinity to oxygen. Similarly to silver, aluminium may perform well as a gate electrode. This has been demonstrated in recent work by M. T. Soo et. al.

Various materials deposited in the form of thick or thin films, are used as the gate oxide in MOS gas sensors. Preliminary studies have been using SiO_2 as the gate oxide. Nonetheless, the lacking of catalytic behaviour in SiO_2 may hamper the gas sensing capability of the MOS gas sensors. Newer development has substituted SiO_2 with high *k* gate oxides, such as ZnO and SnO_2, which are adsorptive and could demonstrate better catalytic behaviour. The analyte gas molecules are first dissociated on the gate electrode surface into atomic gas. Subsequently, the atomic gas diffuses through the electrode and adsorbed at the gate oxide surface. Catalytic behaviour of high *k* gate oxides may further dissociate the atomic gas. The atoms polarize and give rise to a dipole layer, which in turn will change the work function of the gate electrode.

The selection of a suitable high k gate oxide has never been an easy job because it needs to fulfill many requirements, which are comprised of sensitivity, selectivity, and stability in order to achieve long term performance. More fundamental studies are required in order to understand the nature of the gas sensing effect of the high k gate oxide. Nevertheless, present paper is not intended to include exhaustive review of high k gate oxides that have been used as gas sensing material in field-effect MOS gas sensors.

CeO_2 has attracted considerable attention due to its reversible transformation of Ce^{4+} to Ce^{3+} states (redox cycle) that involves oxygen exchange between gas phase O_2 and lattice oxygen. The onset temperature for oxygen exchange in CeO_2 was reported to happen at 600°C, meaning that redox cycle initiates at 600°C. In CeO_2, the highly mobile oxygen anions in octahedral sites of CeO_2 lattice would release from the lattice and form gas phase O_2, leaving oxygen vacancies in the lattice. Formation of these oxygen vacancies is accompanied by transformation of Ce^{4-} to Ce^{3+}. Re-oxidation of Ce^{3+} to Ce^{4+} may happen, favourably in the spacious octahedral sites, wherein the O_2 that has been released would fill the oxygen vacancies, leading to reversed transformation of Ce^{3+} to Ce^{4+}. Apart of these, CeO_2 has been widely investigated as a high k gate oxide on Si, GaN, and 4H-SiC substrates. This is attributed to the high k value (k= 26) and large band gap of CeO_2 (6 eV).

Introduction of an aliovalent cation into CeO_2 lattice may improve the redox property of CeO_2. The trivalent ion, lanthanum (La^{3+}) has been recently introduced into CeO_2 lattice to form lanthanum cerium oxide ($La_xCe_{1-x}O_z$). Addition of La^{3+} alters the CeO_2 structure by introducing more oxygen vacancies in CeO_2 lattice, which increases oxygen exchange and thus favors the redox cycle. Previous literatures reported that a decrease in the onset temperature of oxygen exchange from 600°C to 400°C was reported after the addition of La^{3+} into CeO_2. In addition, amount of Ce^{4+} that can be reduced is enhanced in La^{3+}-doped CeO_2. It has been reported that reduction profile of CeO_2 demonstrated two reduction peaks, which

corresponds to surface and bulk reduction, happening respectively at 429°C and 787°C. Addition of La^{3+} into CeO_2 enhances reducibility of Ce^{4+} to Ce^{3+} by decreasing the onset temperature of bulk reduction to a temperature closer to that of surface reduction. Therefore, addition of La^{3+} into CeO_2 increases amount of oxygen exchange and amount of Ce^{4+} that can be reduced via the introduction of more oxygen vacancies in the lattice.

Furthermore, addition of La_2O_3 into CeO_2 was anticipated to improve the k of the oxide because of the high dielectric polarizability of La^{3+} in La_2O_3. It was reported that they are having a k value of 22–27 for $LaAlO_3$ when compared with Al_2O_3 (k= 8–10) and an increment of k value for HfO_2 and ZrO_2 (k= 20–25) to 38–39 for $La_2Hf_2O_7$ and $La_2Zr_2O_7$. Enhancement of k is also obtained for Lu_2O_3 from 16 to 32 for $LaLuO_3$.

Up-to date, $La_xCe_{1-x}O_z$ has been known for its functions as a thermal barrier coating material, three-way-automotive catalyst, and surrogate material for uranium oxide. Besides, it has been also used as a buffer layer in the development of coated Ni-W conductor. Nevertheless, the application of $La_xCe_{1-x}O_z$ as a metal reactive oxide material and/or high k oxide in MOS based devices has yet to be explored. Therefore, this project aims to investigate $La_xCe_{1-x}O_z$ in terms of its catalytic and insulating properties.

3. Methodology

The lanthanum cerium oxide precursor was prepared as follows. Lanthanum nitrate (Aldrich) and cerium (III) acetylacetonate hydrate (Aldrich) were used as the starting materials. Initially, small amount of cerium acetylacetonate hydrate powder was dissolved in 3 ml of methanol (J. T. Baker, Analytical grade), followed by an addition of a few drops of acetic acid (J. T. Baker, CMOS grade) to obtain a 0.25 M cerium-containing precursor solution. The mixture was then stirred continuously for 15 min. The lanthanum nitrate powder was converted to lanthanum acetylacetonate by dissolving an appropriate amount of

the powder in acetylacetone to make up lanthanum-containing precursor solution. Similarly, this solution was continuously stirred for 15 min and subsequently added to the cerium containing precursor solution and stirred for another 15min. After a homogeneous mixture was produced, it was then refluxed for 2 h. The resulting lanthanum cerium oxide precursor was allowed to cool prior to spin-coating on a 1-cm^2 cleaned n-type Si (100) and 4H-SiC (0001) substrates. Then, the samples were inserted into a horizontal tube furnace for post-deposition annealing with a heating rate of 5°C/min. The samples were then cooled down slowly at a rate of 5°C/min. In order to fabricate the MOS structures, aluminum (Al) was evaporated on the $La_xCe_{1-x}O_z$ using thermal evaporator (AUTO 306). Then, an array of Al gate electrodes (area= 0.0025 cm^2) was defined using photolithography process. Subsequently, the back of the substrates was coated with a layer of Al. Thereafter, capacitance-voltage (*C-V*) and current-voltage (*I-V*) characteristics of the metal-oxide-semiconductor (MOS) test structure were tested using inductance-capacitance-resistance (LCR) meter (Agilent 4248A) and semiconductor parameter analyzer (Agilent 4156C), respectively.

4. Results

(I) Deposition of $La_xCe_{1-x}O_z$ on Si substrate

(a) Effects of post-deposition annealing temperature (400-1000°C)

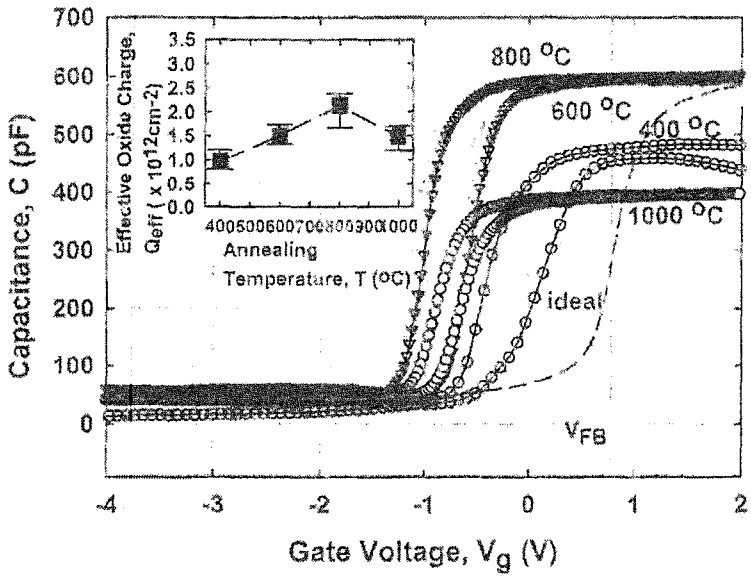

Fig. 1 Typical high frequency capacitance-voltage (*C-V*) curves of samples annealed at different annealing temperatures (400-1000°C) for a 15 minutes dwell time. An ideal *C-V* curve is indicated by a dashed-line and a vertical solid line indicates the V_{FB}. Inset shows the relationship between effective oxide charges and annealing temperature. The error bars indicate the maximum, average, and minimum values of the investigated parameters.

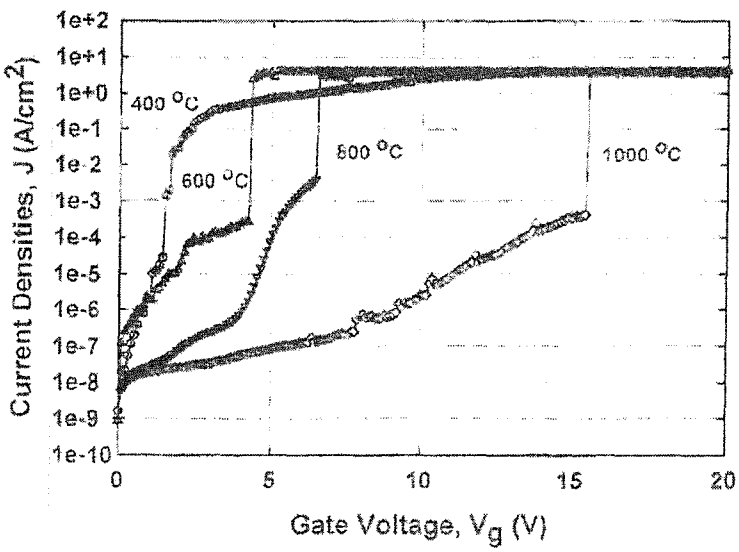

Fig. 2 Leakage current density-gate voltage characteristics of Al/$La_xCe_{1-x}O_7$/Si MOS capacitor at different annealing temperatures (400-1000°C) for 15 minutes.

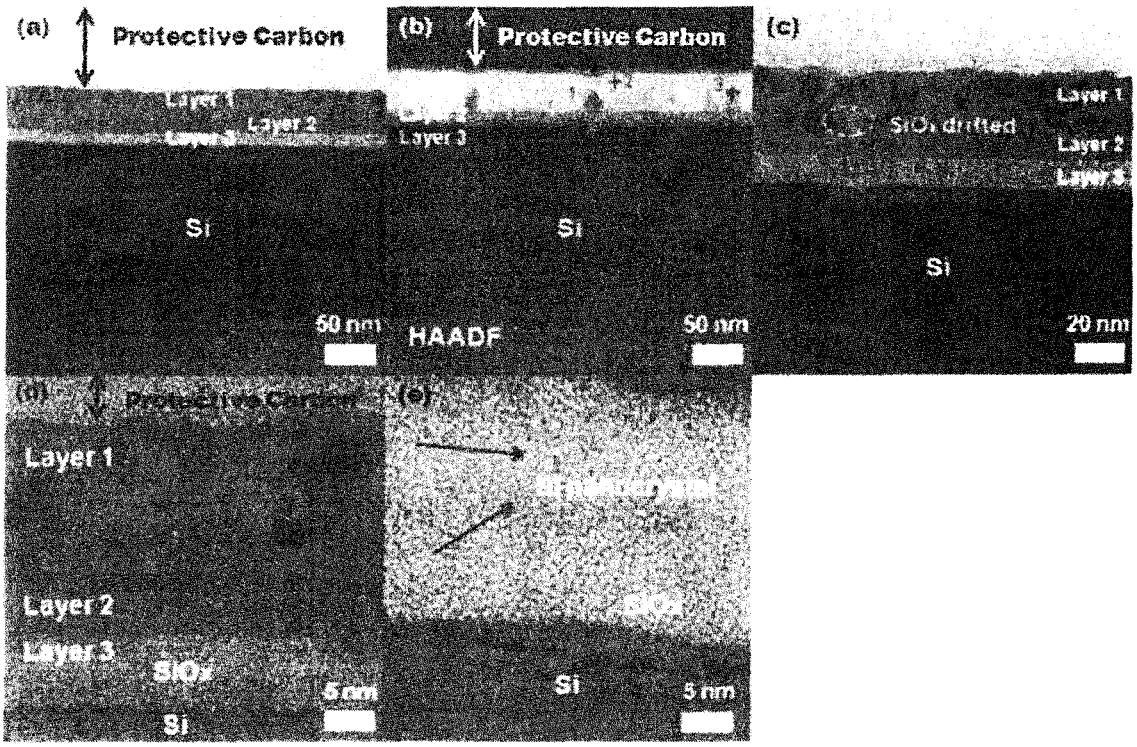

Fig. 3 Cross sectional high resolution transmission electron microscopy images of sample annealed at 1000°C for 15 minutes.

(b) Effects of post-deposition annealing time (15, 30, 60, 120 min)

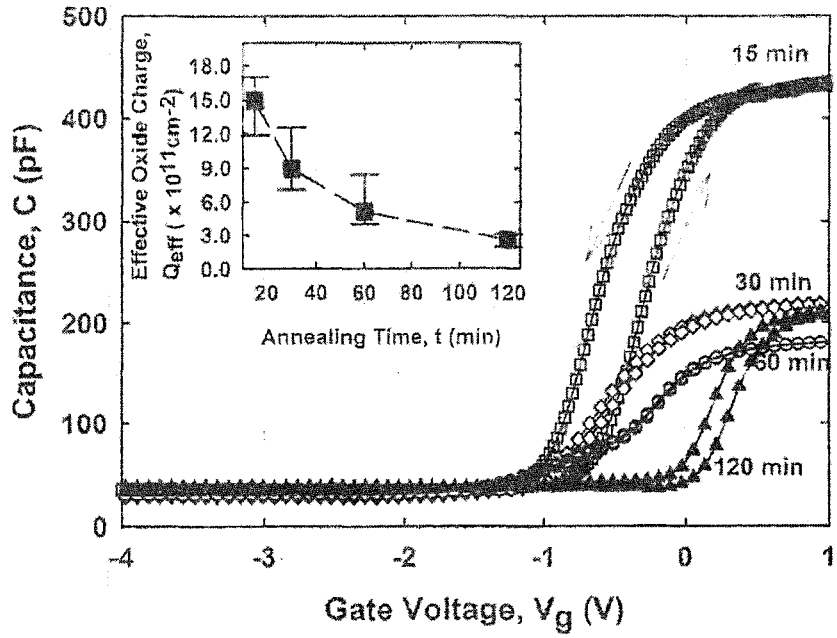

Fig. 4 Typical high frequency capacitance-voltage (C-V) curves of samples annealed at 1000°C for different annealing time (15-120 minutes). Inset shows the relationship between effective oxide charges in error bars with annealing time.

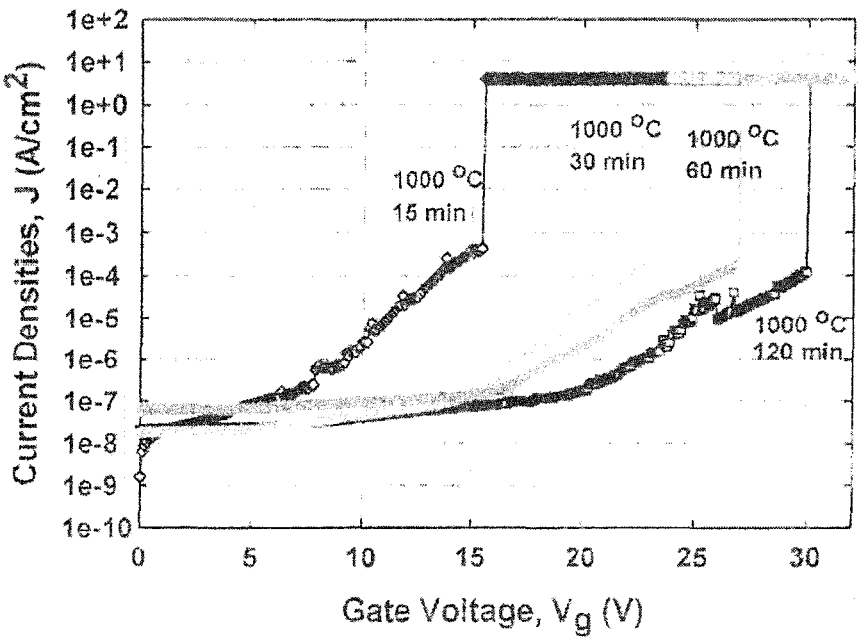

Fig. 5 Leakage current density-gate voltage characteristics of Al/$La_xCe_{1-x}O_z$/Si MOS capacitor at different annealing time (15-120 minutes) for the 1000°C-annealed sample.

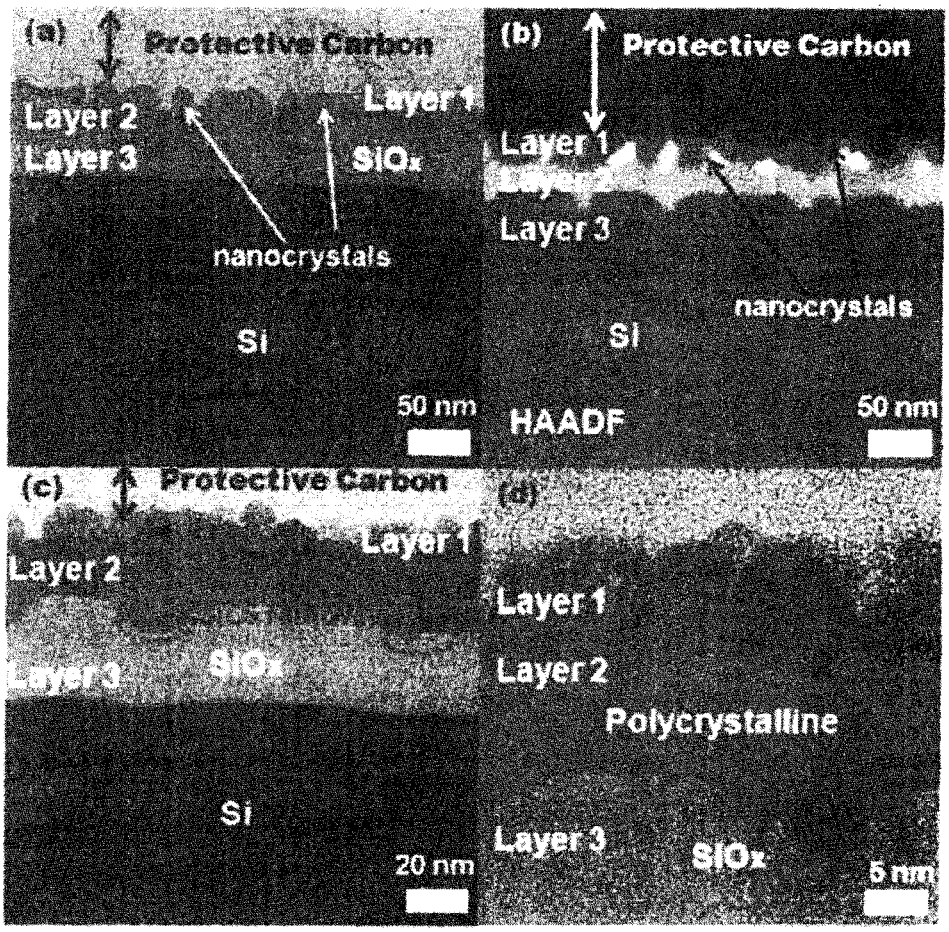

Fig. 6 Cross sectional high resolution transmission electron microscopy images of sample annealed at 1000°C for 120 minutes.

(c) Effects of spin coating rates (3000, 4000, 5000 rpm)

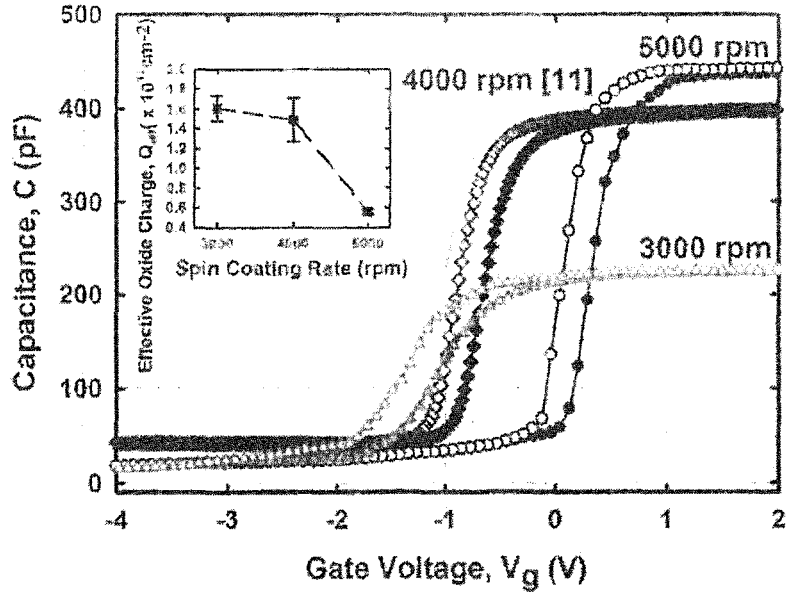

Fig. 7 High frequency capacitance-voltage (*C-V*) curves and effective oxide charges (inset) of interface trap density (inset) of samples spin-coated at different spin coating rates (3000-5000 rpm).

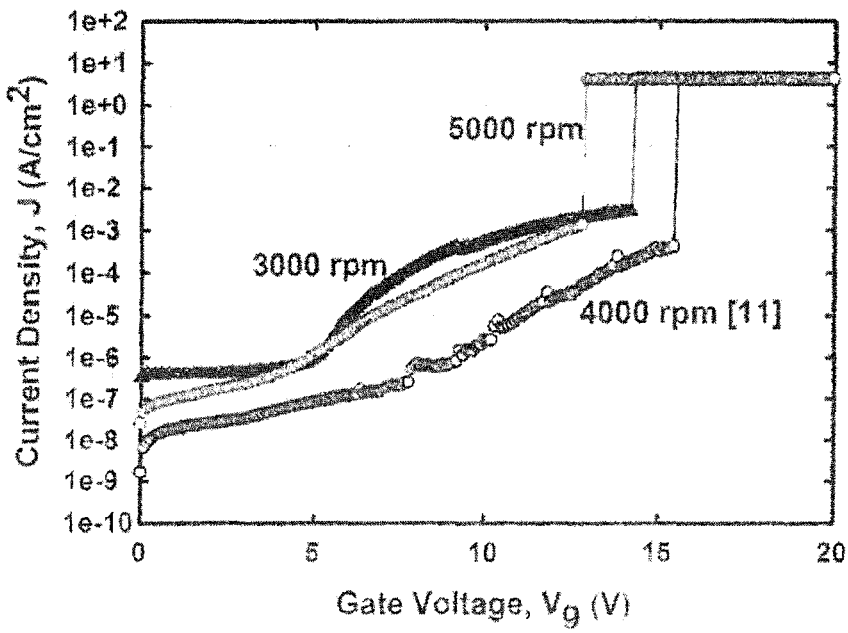

Fig. 8 Leakage current density-gate voltage (J-V_g) characteristics of samples spin-coated at different spin coating rates.

(d) Effects of molar ratios of La:Ce (1:1, 1:0.75, 1:0.50, 1:0.25)

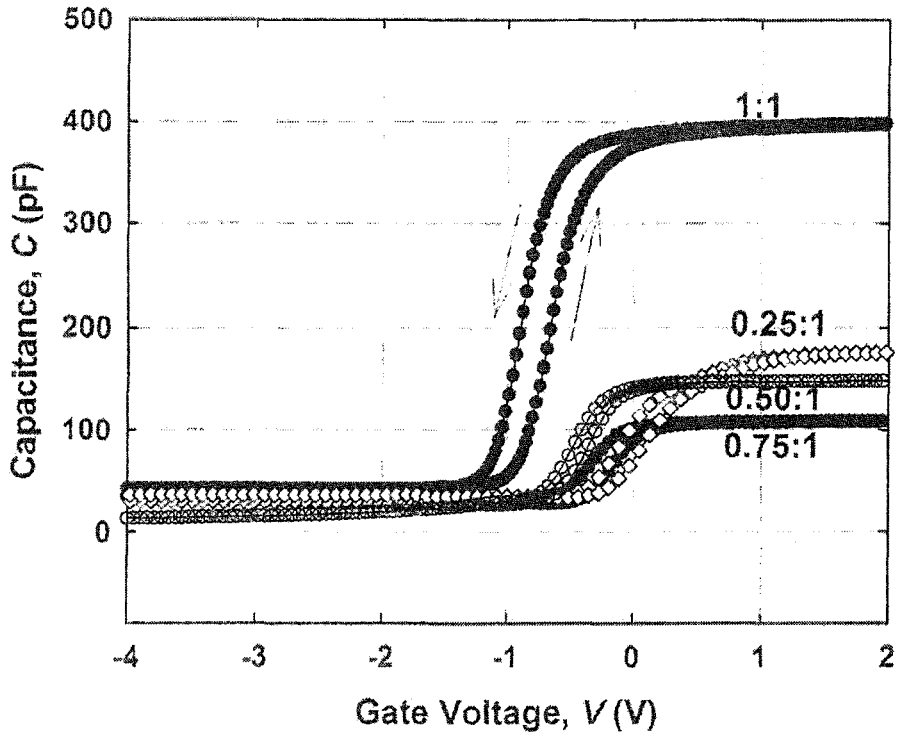

Fig. 9 Capacitance-gate voltage characteristics of Al/$La_xCe_{1-x}O_z$/Si samples prepared using 0.25:1, 0.50:1, 0.75:1, and 1:1 molar ratios.

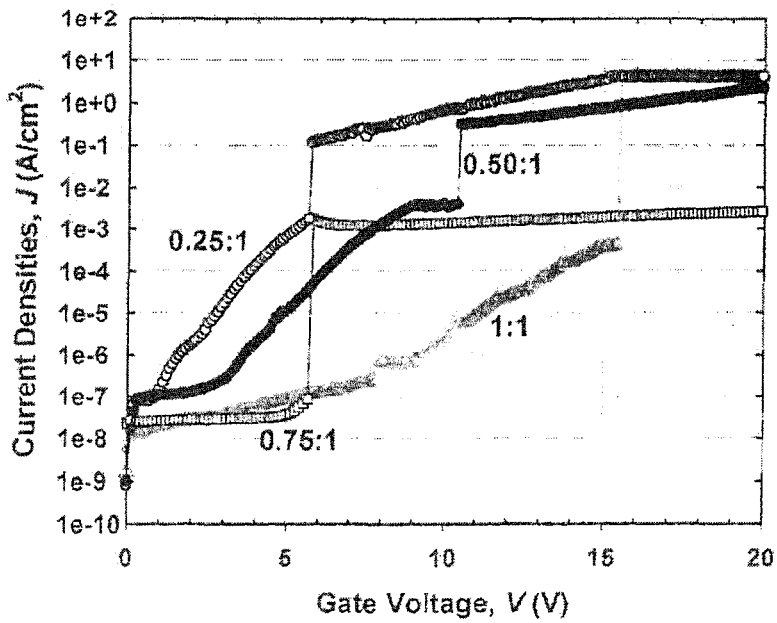

Fig. 10 Current densities-gate voltage (*J-V*) behaviors of Al/$La_xCe_{1-x}O_z$/Si structure with different molar ratios of La:Ce

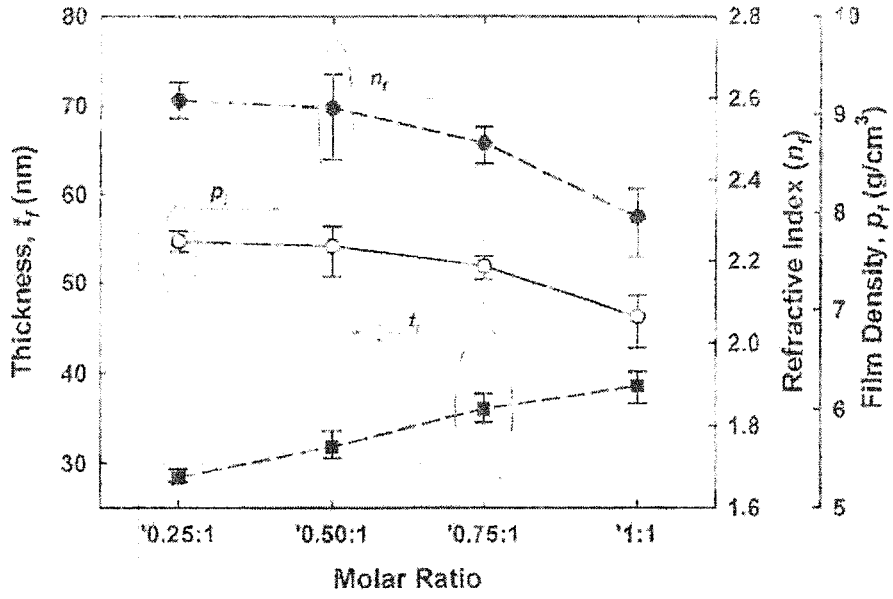

Fig. 11 A relationship between film thickness, refractive index, and film density as a function of molar ratio.

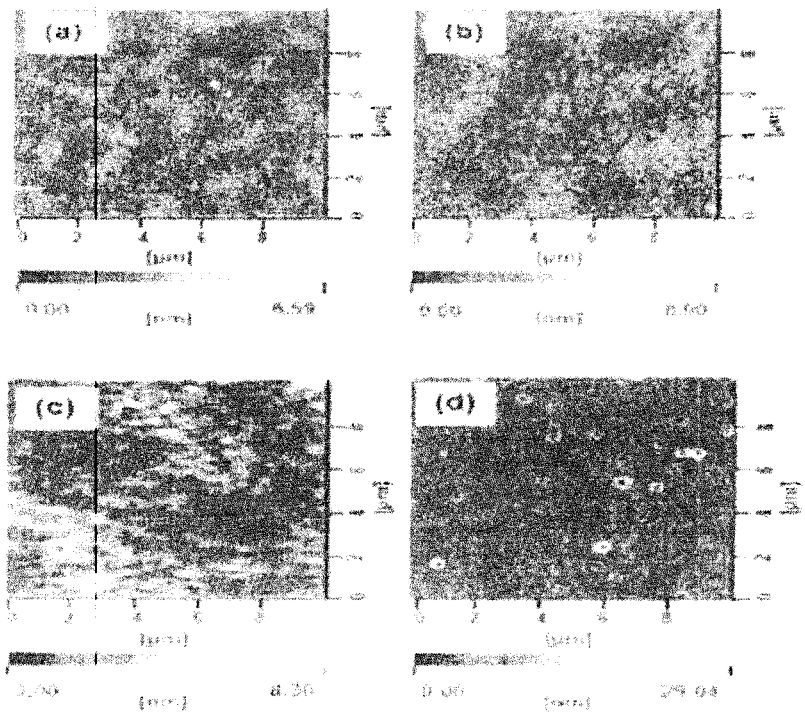

Fig. 12 Atomic force microscopy surface topography of $La_xCe_{1-x}O_z$ film in (a) 0.25:1, (b) 0.50:1, (c) 0.75:1, and (d) 1:1 molar ratios.

(e) Sensing performance of Al/$La_xCe_{1-x}O_z$/Si structure

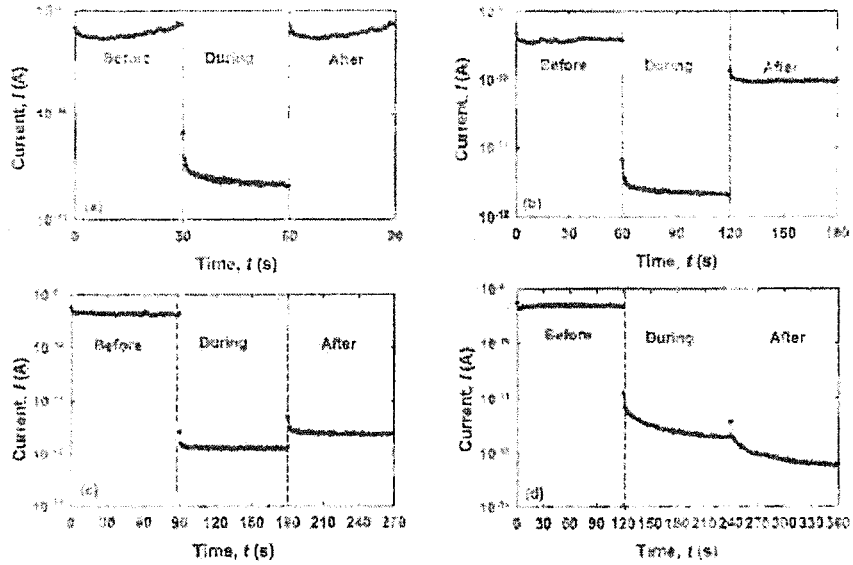

Fig. 13 Current-time (*I-t*) characteristics of Al/$La_xCe_{1-x}O_z$/Si as a function of (a) 0.25:1, (b) 0.50:1, (c) 0.75:1, and (d) 1:1 molar ratios.

(II) Deposition of $La_xCe_{1-x}O_z$ on 4H-SiC substrate

(a) Effects of post-deposition annealing temperature (400-1000°C)

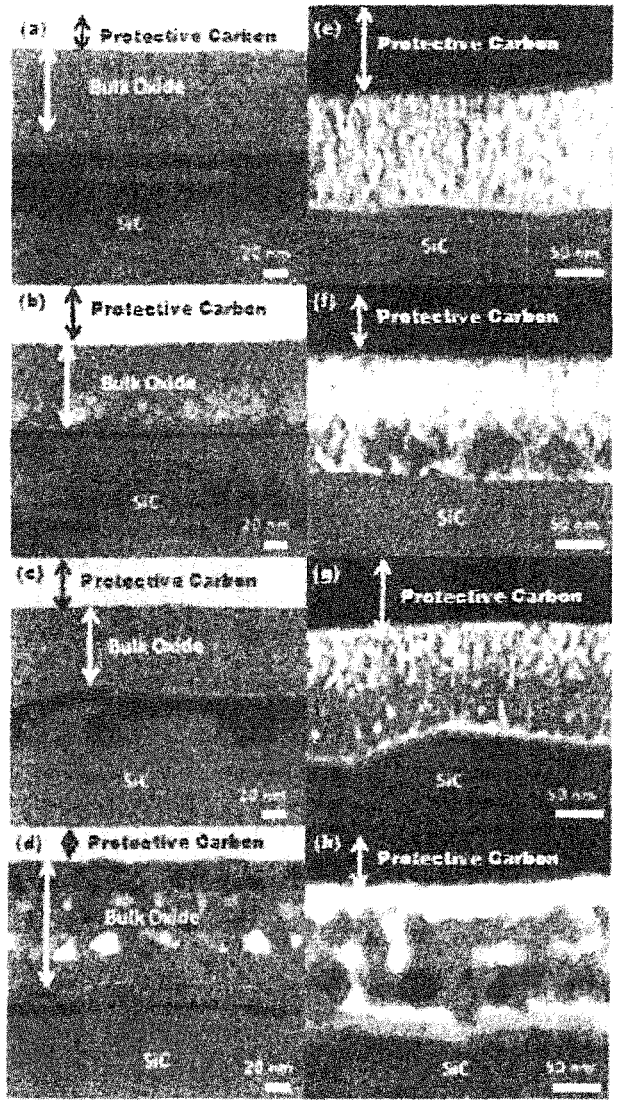

Fig. 1 Cross sectional high resolution transmission electron microscopy (HRTEM) bright field [(a)-(d)] and high-annular angle dark field (HAADF) [(e)-(h)] images of samples annealed at 400°C [(a) and (e)], 600°C [(b) and (f)], 800°C [(c) and (g)], and 1000°C [(d) and (h)].

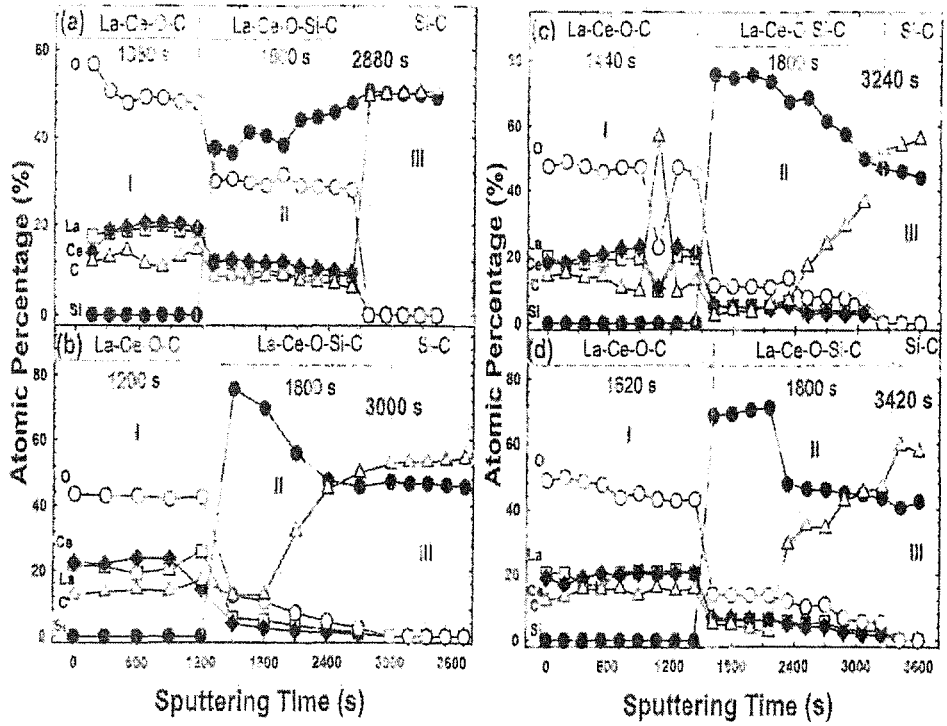

Fig. 2 XPS depth profiles of samples annealed at (a) 400°C, (b) 600°C, (c) 800°C, and (d) 1000°C.

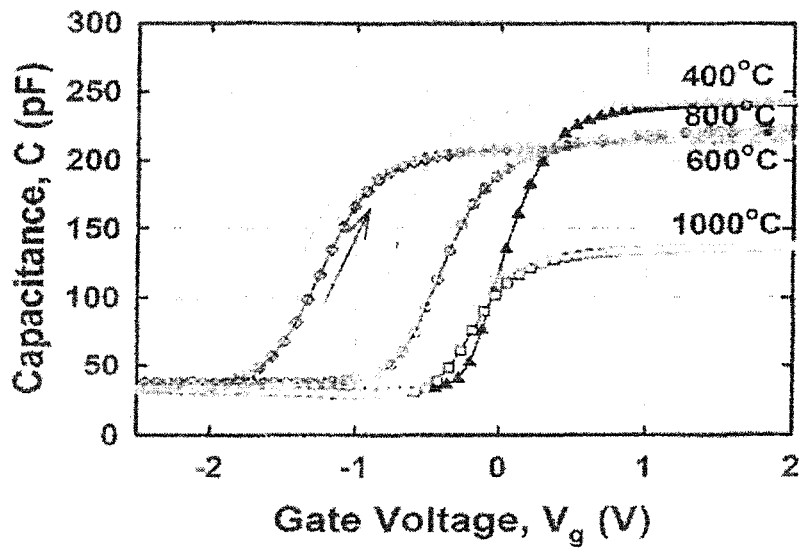

Fig. 3 High frequency (1 MHz) capacitance-voltage characteristics of samples annealed from 400 to 1000°C.

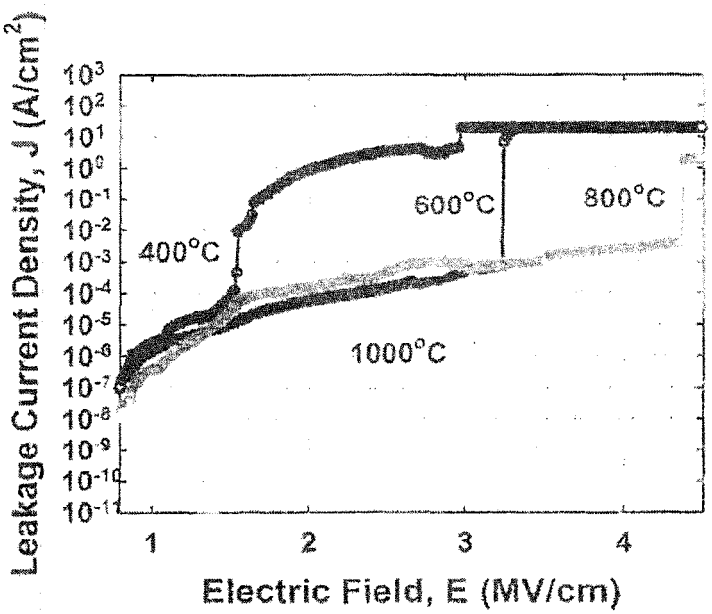

Fig. 4 Leakage current density-electric field (J-E) characteristics of oxides annealed from 400 to 1000°C.

(b) Effects of post-deposition annealing time (15, 30, 60, 120 min)

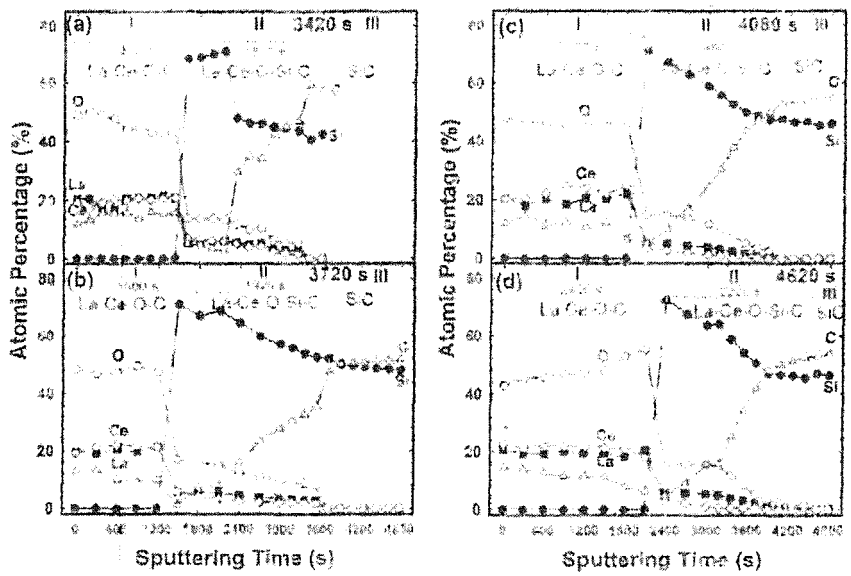

Fig. 5 XPS depth profiles of samples annealed at 1000°C for (a) 15 min, (b) 30 min, (c) 60 min, and (d) 120 min.

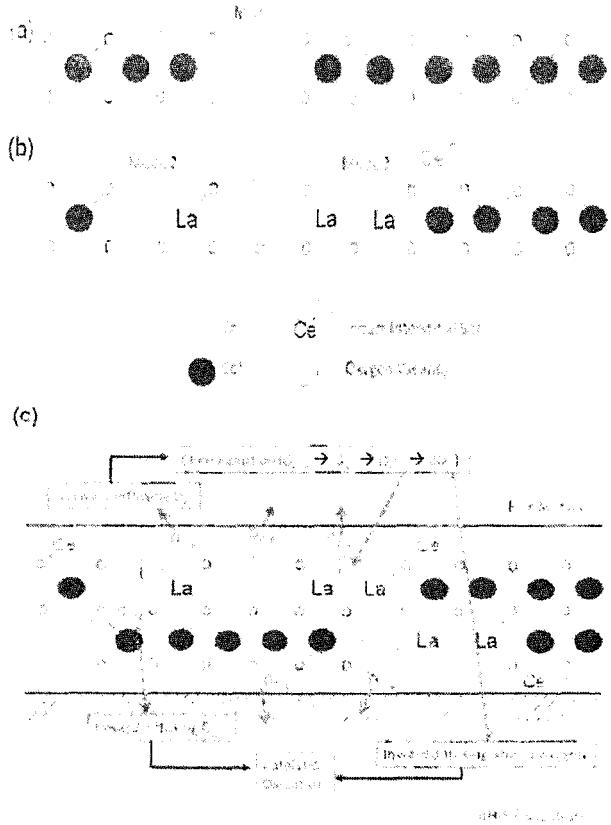

Fig. 6 Schematic diagram showing (a) intrinsic oxygen vacancies, (b) oxygen vacancies after addition of La^{3+}, and (c) corresponding $La_xCe_{1-x}O_z$ solid solution. Solid arrows indicate outward diffusing O_2 while dashed arrows indicate inward diffusing O_2 and/or absorbed oxygen atoms.

(c) Effects of molar ratios of La:Ce (1:1, 1:0.75, 1:0.50, 1:0.25) *On going*

(d) Effects of post-deposition annealing ambient (Ar, O_2, N_2, 95%N_2-H_2) *On going*

(e) Sensing performance of Al/$La_xCe_{1-x}O_z$/4H-SiC structure *On going*

5. DISCUSSION

Both the catalytic and insulating properties of $La_xCe_{1-x}O_z$ as metal reactive oxide and high dielectric constant oxide have been successfully addressed, respectively in this project. It was deduced that amount of oxygen vacancies present in $La_xCe_{1-x}O_z$ was enhanced significantly as a result of substitution of Ce^{4+} cation in CeO_2 lattice by La^{3+} cation. Apart from the intrinsic oxygen vacancies in CeO_2, two additional oxygen vacancies will be formed upon substitution of Ce^{4+} in CeO_2 by La^{3+}. Substitution of one Ce^{4+} cation by one La^{3+} cation gives rise to one oxygen vacancy and the adjacent Ce^{4+} cation is reduced to Ce^{3+}. Charge balance is accomplished by creating one oxygen vacancy when two adjacent Ce^{4+} cations are reduced to Ce^{3+}. The formation of oxygen vacancies is due to the removal of the oxygen anion (O^{2-}) from its position in the CeO_2 lattice when La^{3+} takes the place of Ce^{4+}. The displaced Ce^{4+} will reside at the interstitial site, forming Ce^{4+} interstitials. The floating O^{2-} anions, which carry two electrons, tend to donate the two electrons and form oxygen gas (O_2). The two electrons will be consumed by neighbouring Ce^{4+} to reduce to Ce^{3+}. The resulting O_2 will either diffuse outward to the film surface or inward to the oxide-4H-SiC interface. O_2 that is diffusing outward will be re-captured by $La_xCe_{1-x}O_z$ because $La_xCe_{1-x}O_z$ itself can act as a catalyst. Similarly when $La_xCe_{1-x}O_z$ is utilized in MOS gas sensors and exposed to O_2 as the sensing gas, the O_2 gas molecules will be captured by $La_xCe_{1-x}O_z$. This is because the presence of oxygen vacancies in $La_xCe_{1-x}O_z$ may act as the active sites for the absorption of O_2. Chemisorption happens when the O_2 are absorbed to atomic oxygen species. In addition, the presence of oxygen vacancies in the lattice favours migration of neighbouring O^{2-}. This has enhanced the oxygen mobility in the oxide. Meanwhile, filling of oxygen vacancies can also happen, in which some of the atomic oxygen species will combine with the oxygen vacancies. This filling process will cause the adjacent Ce^{3+} to re-oxidize back to Ce^{4+}. Re-

oxidation of Ce^{3+} to Ce^{4+} shrinks the lattice because of smaller ionic radius of Ce^{4+} (0.097 nm) than Ce^{3+} (0.110 nm), and thus decrease the crystallite size of $La_xCe_{1-x}O_z$ in this work.

Electrical performance of $La_xCe_{1-x}O_z$ as the high dielectric constant gate oxide and sensing behaviours of $La_xCe_{1-x}O_z$ as the metal reactive oxide in MOS based structures has been studied in this project. Nevertheless, in current stage, conduction mechanism that may influence both the electrical and sensing behaviours of the samples have not been extracted at this moment because detailed study in different types of conduction mechanisms are necessary and much time is required to calculate for different parameters that can be extracted from the different types of conduction mechanisms as well as to correlate the respective mechanism with the electrical and sensing behaviours of the samples. In order to perform this, we need to use computer software that can help us to fit the leakage current-gate voltage curves with respective conduction mechanisms that were built up with mathematical equations. This software ought to be purchased or else studies of conduction mechanism cannot be undergone. However, with the limited budget leftover, alternative route is to be looked for.

6. OUTCOME/OUTPUT OF RESEARCH

[1] W. F. Lim, K. Y. Cheong, and Z. Lockman. Effects of post-deposition annealing temperature and time on physical properties of metal-organic decomposed lanthanum cerium oxide thin film, Thin Solid Films 519 (2011) 5139-5145.

[2] W. F. Lim, Z. Lockman, and K. Y. Cheong, Influence of Post-Deposition Annealing on Metal-Organic Decomposed Lanthanum Cerium Oxide Film, Proceedings of IEEE (2011) 24-27.

[3] W. F. Lim, Z. Lockman, and K. Y. Cheong. Metal-oxide-semiconductor characteristics of lanthanum cerium oxide film on Si, Applied Physics A 107 (2012) 459-467.

[4] W. F. Lim, Z. Lockman, and K. Y. Cheong, Influence of spin coating rate on metal-organic decomposed lanthanum cerium oxide film on Si substrate, *Submitted to World Applied Science Journal* (2013).

[5] W. F. Lim, H. J. Quah, and K. Y. Cheong, Kesan suhu penyepuhlindapan terhadap sifat-sifat elektrikal filem $La_xCe_{1-x}O_z$ terendap pada silicon, *Submitted to Jurnal Teknologi (Sciences & Engineering)* (2013).

[6] W. F. Lim, Z. Lockman, and K. Y. Cheong, Investigation of $La_xCe_yO_z$ as a High-Dielectric Constant Metal Reactive Oxide on Si Substrate, *Accepted for Publication in Physics Express* (2013).

[7] W. F. Lim and K. Y. Cheong, Influence of post-deposition annealing time on metal-organic-decomposed $La_xCe_{1-x}O_z$ as a catalytic oxide on 4H-SiC substrate, *Submitted to Physical Chemistry Chemical Physics* (Under Review-2013).

[8] W. F. Lim, Z. Lockman, and K. Y. Cheong, Study of molar ratio on the characteristics of metal-organic decomposed $La_xCe_{1-x}O_z$film as a metal reactive oxide on Si substrate, *Submitted to Journal of Inorganic and Polymeric Materials* (Under Review-2013).

[9] W. F. Lim and K. Y. Cheong, Effects of Post-Deposition Annealing Temperature on Metal-Organic Decomposed Lanthanum Cerium Oxide Film as Metal Reactive Oxide Layer on 4H-SiC, *Submitted to Materials Chemistry and Physics (Responding to Reviewers' Comment-present).*

[10] W. F. Lim and K. Y. Cheong, Effects of Post-Deposition Annealing Temperature on Band Alignment and Electrical Characteristics of Lanthanum Cerium Oxide on 4H-SiC, Materials Research Society Symposium Proceedings 1433 (2013) 1-6, DOI: 10.1557/opl.2012.1144.

7. Executive Summary

Objectives, which have been achieved included

(a) To study effects of post-deposition annealing (temperature, time, and ambient),

(b) To study effects of spin coating rate, and

(c) To study effects of varying molar ratios

onto $La_xCe_{1-x}O_7$ have been successfully investigated in this project.

As a conclusion, results obtained from this project have justified the potential of utilizing $La_xCe_{1-x}O_7$ as a metal reactive oxide in MOS based gas sensor and also as a high dielectric constant gate oxide material in MOS based devices.

Prepared by,

Lim Way Foong

Certification/Verification of Report,

Assoc. Prof. Ir. Dr. Cheong Kuan Yew

ASSOC. PROF. IR. DR. CHEONG KUAN YEW
Universiti Sains Malaysia
Engineering Campus
School of Materials & Mineral Resources Engineering
14300 Nibong Tebal,
Penang, Malaysia.